

Tetrameric 1:1 and monomeric 1:3 complexes of silver(I) halides with tri(*p*-tolyl)-phosphine: A structural and biological study

Sotiris Zartilas^a, Sotiris K. Hadjikakou^{a,*}, Nick Hadjiliadis^{a,*}, Nikolaos Kourkoumelis^a, Loukas Kyros^a, Maciej Kubicki^b, Martin Baril^c, Ian S. Butler^c, Spyros Karkabounas^d, Jan Balzarini^e

^a Section of Inorganic and Analytical Chemistry, Department of Chemistry, University of Ioannina, 45110 Ioannina, Greece

^b Department of Chemistry, A. Mickiewicz, University, ul. Grunwaldzka 6, 60-780 Poznan, Poland

^c Department of Chemistry, McGill University, 801 Sherbrooke, Montreal Quebec, Canada H2A 2K6

^d Department of Experimental Physiology, Medical School, University of Ioannina 45110 Ioannina, Greece

^e Katholieke Universiteit Leuven, Rega Institute for Medical Research, Minderbroedersstraat 10, B-3000 Leuven, Belgium

Received 8 March 2007; received in revised form 13 July 2007; accepted 25 July 2007

Available online 9 August 2007

Dedicated to Bernhard Lippert.

Abstract

Silver(I) halides react with tri(*p*-tolyl)phosphine (tptp, C₂₁H₂₁P) in MeOH/MeCN solutions in 1:1 or 1:3 molar ratios to give complexes of formulae {[AgCl(tptp)]₄} (**1**) or [AgX(tptp)₃] (X = Cl (**2**), Br (**3**), I (**4**)), respectively. The complexes were characterized by elemental analyses, and FT-IR far-IR, FT-Raman, TG and ¹H, ¹³C, ³¹P NMR spectroscopic techniques. Crystal structures of complexes **2–4** were determined by X-ray diffraction at room temperature (rt). The crystal structure of **1** and **4** was also determined at 100(1) and 140(2) K (lt), respectively. In complex **1** four μ₃-Cl ions are bonded with four Ag(I) ions forming a cubane while the coordination sphere of silver(I) ions is completed by one P atom from a terminal tri(*p*-tolyl)phosphine ligand. In complexes **2–3** one terminal halogen and three P atoms from phosphine ligands form a tetrahedral arrangement around the metal ion. Complexes **1–4** were tested for *in vitro* cytostatic activity against sarcoma cancer cells (mesenchymal tissue) from the Wistar rat, polycyclic aromatic hydrocarbons (PAH, benzo[*a*]pyrene) carcinogenesis and against murine leukemia (L1210) and human T-lymphocyte (Molt4/C8 and CEM) cells. The silver(I) complexes **1–4** show strong activity.

© 2007 Elsevier B.V. All rights reserved.

Keywords: Bioinorganic chemistry; Silver(I) complexes; Tri(*p*-tolyl)phosphine; Crystal structures; Cytostatic activity

1. Introduction

The ability of silver(I) complexes to adopt geometries with variable nuclearities and structural diversity makes the study of silver(I) chemistry very attractive [1]. Such silver(I) complexes exhibit a wide range of applications in medicine, in analytical chemistry or in industry of poly-

mers [1]. Especially, the biomedical applications and uses of silver(I) complexes are related to their antibacterial action [2], which appears to involve interaction with DNA [3]. Also, it has been shown that Ag(I) ions exterminate almost instantaneously the microbes by stopping the thoroughfare of breathing of cells [4]. Recently, Ag(I) thioamide complexes have been studied for their antitumor activity [5]. The mechanism of anti-tumor action of Ag(I) compounds is still unknown. It is well known, however, that many drugs, which inhibit the growth of tumor cells act either by interfering with the bases and/or nucleotides of the double helix of DNA or with the metalloenzymes

* Corresponding authors. Tel.: +30 26510 98374 (S.K. Hadjikakou), tel.: +30 26510 98420; fax: +30 26510 98786 (N. Hadjiliadis).

E-mail addresses: shadjika@uoi.gr (S.K. Hadjikakou), nhadjil@uoi.gr (N. Hadjiliadis).

that are necessary for the rapid growth of malignant cells [6].

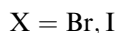
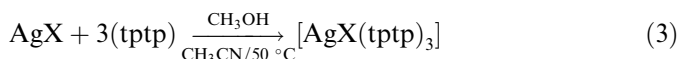
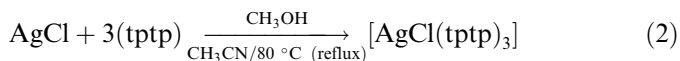
The ligand tri(*p*-tolyl)phosphine was chosen for the preparation of new Ag(I) complexes expected to possess biological activity. The known phosphine complexes of metal with applications in medicine is auronofin (tri-ethyl-phosphine-gold(I) thioglucose (Et₃PAuTg)) and its second generation drug Ridaura TM (tri-ethyl-phosphine (2,3,4,6-tetra-acetyl-glycopyrasonato-*S*)-gold(I) (Et₃PauSATg)), an extensively gold(I) anti-arthritic drug in use, which contain phosphine [2a]. This complex was found to be highly cytostatic to tumour cells and active against i.p. P388 leukaemia [7a,7b,7c,7d,7e]. Sadler et.al. [7f], have studied the effect of auranofin complexes in the growth of *Pseudomonas putida*.

This paper, reports the synthesis and structural characterization of four new silver complexes with tri(*p*-tolyl)phosphine of formulae {[AgCl(tptp)]₄} (**1**); [AgCl(tptp)₃] (**2**); [AgBr(tptp)₃] (**3**) and [AgI(tptp)₃] (**4**). Complexes **1–4** were tested for *in vitro* cytostatic activity against sarcoma cancer cells (mesenchymal tissue) from the Wistar rat, polycyclic aromatic hydrocarbons (PAH, benzo[*a*]pyrene) carcinogenesis and against murine leukemia (L1210) and human T-lymphocyte (Molt4/C8 and CEM) cells.

2. Results and discussion

2.1. General aspects

The synthesis of complexes **1–4** was carried out in CH₃OH/CH₃CN (1:1) [8] according to the reactions shown below:



Metal conductance (A_m) values of the complexes in CH₃CN solutions are 1–14 (cm⁻¹ mol⁻¹ Ω⁻¹) showing that the complexes are not conducting in solution. The geometry around silver(I) ions in all complexes is tetrahedral. Complex **1** adopts a tetramer cubane configuration, which consist of Ag–P bridged by μ₃-Cl atoms, while complexes **2–4** have a monomer tetrahedral structure with the general formula AgP₃X (X = Cl, Br, I). The formulae of complexes **1–4** were first deduced by elemental analyses and spectroscopic data. Crystals of the complexes are stable in air but were kept in darkness. Complexes **1–4** were soluble in CH₃Cl, DMSO, CH₃CN and CH₃OH.

The crystal structure of complex **4** at 293(2) K has been also reported elsewhere [8e] but we repeat its structure determination here at 140(2) K in order to investigate the influence of low temperature in crystal packing. This crystal structure was also re-determined at room temperature

(293(2) K), for comparison but the results were exactly the same with the ones already published [8e].

2.2. Thermal analysis

Thermal analysis in flowing nitrogen shows that complex **1** decomposes with one step at 233–315 °C; with 66.8% endothermic mass loss, which is attributed to the loss of four ligand molecules. Also the same feature is observed in thermographs of complexes **3** and **4**, which decomposed at 188–362 °C with 81.3% mass loss of three ligand molecules in case of **3** and at 200–367 °C with 80.2% mass loss in case of **4**.

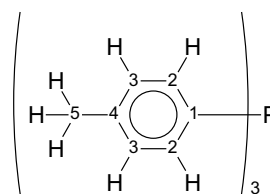
The thermograph of complex **2**, however, shows a two-step decomposition, one with mass loss of 54.6%, which is assigned to the loss of two ligand molecules at 200–320 °C and a second with mass loss of 26.5% of its weight, corresponding to the mass of the third ligand.

2.3. Spectroscopy

2.3.1. Vibrational spectroscopy

The infrared spectra of complexes **1–4**; show distinct vibrational bands at 1097 cm⁻¹ in **1**, 1095 cm⁻¹ **2**, 1095 cm⁻¹ **3** and 1092 cm⁻¹ in **4**; which were tentatively assigned to the symmetric vibrations of the ν(C–P) bond [9a] and at 512, 502 cm⁻¹ **1**; 515, 507 cm⁻¹ **2**; 515, 507 cm⁻¹ **3** and 510, 499 cm⁻¹ **4** [9a,9b]; to the anti-symmetric vibrations. The corresponding ν(C–P) bands of the free tri-*p*-tolylphosphine ligand are found at 1089 cm⁻¹ for the symmetric vibration and at 516 cm⁻¹, 505 cm⁻¹ for the anti-symmetric. The slight shifts towards higher frequencies of the symmetric vibrations of the ν(C–P) in the spectra of complexes **1–4** as compared to the corresponding bands of the free ligand, can be explained either by the shift of π-electron density from the benzene ring to the unfilled d-orbitals of the ligand donor atom (phosphorus) or by the back donation of electron density from the filled d-orbitals of the metal to the vacant d-orbitals of the ligand through d–d, bonding. Both these tendencies strengthen the P–C bond and hence instead of a decrease, a slight increase in ν(P–C) is noticed [9a].

The bands at 186 and 136 cm⁻¹ in case of complex **1**; at 172 cm⁻¹ in **2**; at 135 cm⁻¹ in **3** and at 125 cm⁻¹ in **4** were assigned to the vibrations of the Ag–X bonds, respectively (X = Cl, Br, I) [9c]. The presence of two vibrations for the Ag–Cl bonds in case of complex **1** is due to the unequal Ag–Cl bond distances for the μ₃-Cl bridging atoms in con-



Scheme 1.

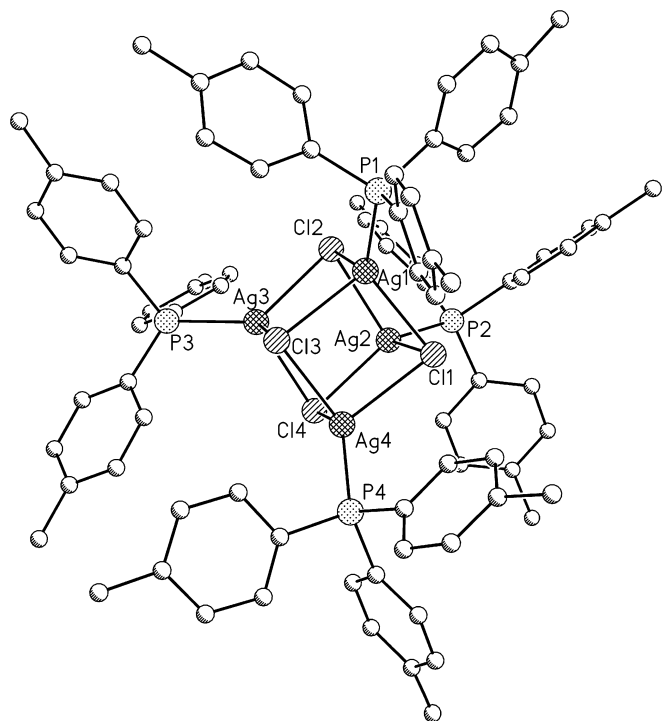


Fig. 1. Molecular diagram of the crystal structure of complex 1.

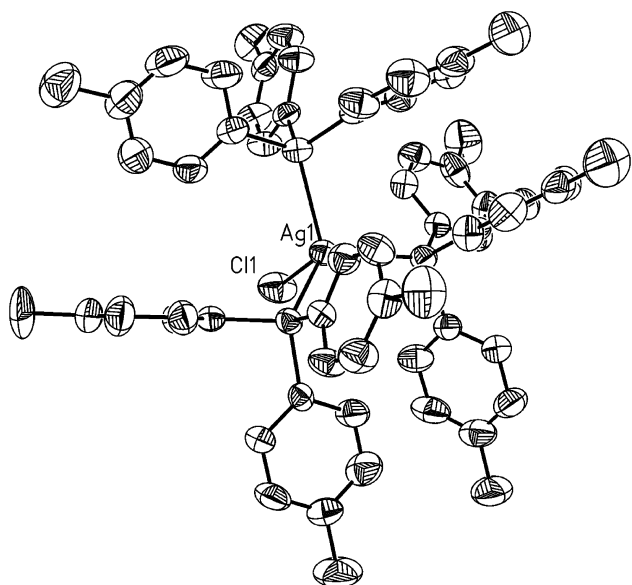


Fig. 2. Molecular diagram of the crystal structure of complex 2.

trast to the terminal chloride ions of the complexes 2–4 (see crystal structures).

The Raman spectra show vibrational bands at 490 cm^{-1} for complex 1 and at 502 and 511 cm^{-1} for 2, which were assigned as the vibrations of the Ag–P bonds [10a,10b]. The presence of two bands for the Ag–P bond stretching vibrations in case of complex 2 indicate two unequal Ag–P bonds in the complex, in accordance with the findings from TGA-DTA analysis described previously for this complex.

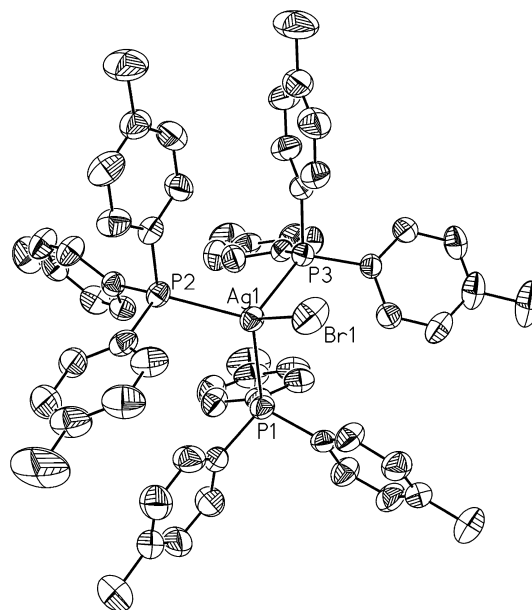


Fig. 3. Molecular diagram of the crystal structure of complex 3.

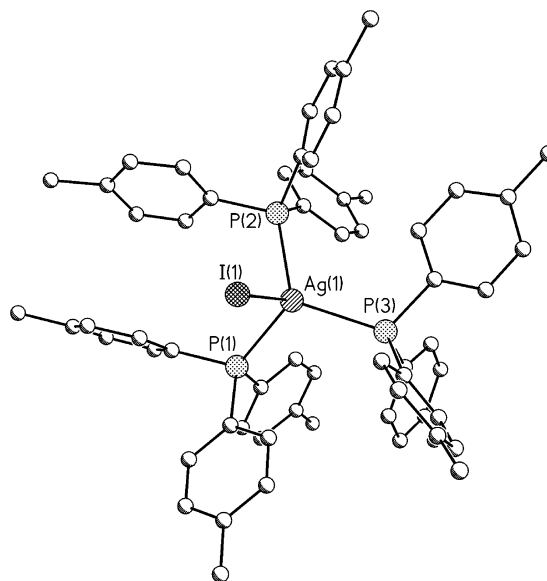


Fig. 4. Molecular diagram of the crystal structure of complex 4.

2.3.2. NMR spectroscopy

The ^1H NMR spectrum of the free ligand tptp (Scheme 1) in CDCl_3 solution shows a resonance signal at 2.36 ppm for the $\text{H}(\text{C}_5)$ protons of the methyl groups and at 7.14 ppm and at 7.27 ppm for the aromatic $\text{H}(\text{C}_2)$ and $\text{H}(\text{C}_3)$ protons of the ligand, respectively. These last two signals are shifted at 7.06 ppm in complex 1; at 7.03 ppm in 2; at 7.07 ppm in 3 and 4 indicating coordination of the ligand to the metal ion.

The ^{13}C NMR spectra of the free ligand shows a peak at 139.24 ppm that is assigned to C_1 . This peak undergoes the most significant shifts of all and appears at 140.51 ppm in 1; at 139.55 ppm in 2; at 139.70 ppm in 3 and at

Table 1
Selected bond lengths (Å) and angles (°) for the compounds **1–4** with e.s.d.'s in parentheses

1 at 293 K		2 at 293 K		3 at 293 K		4 at 293 K		4 at 140 K	
Ag1–Cl1	2.566(8)	Ag1–Cl1	2.6186(17)	Ag1–Br1	2.7050(6)	Ag1–I1	2.8655(9)	Ag1–I1	2.8736(6)
Ag1–Cl2	2.622(9)	Ag1–P1	2.5566(12)	Ag1–P1	2.5545(10)	Ag1–P1	2.5294(17)	Ag1–P1	2.5208(15)
Ag1–Cl3	2.735(7)	Ag1–P2	2.5347(11)	Ag1–P2	2.5367(10)	Ag1–P2	2.558(2)	Ag1–P2	2.5453(15)
Ag2–Cl1	2.807(8)	Ag1–P3	2.5609(11)	Ag1–P3	2.5624(10)	Ag1–P3	2.5529(17)	Ag1–P3	2.5444(13)
Ag2–Cl2	2.697(9)	Cl1–Ag1–P1	108.88(5)	Br1–Ag1–P1	109.39(3)	I1–Ag1–P1	102.37(5)	I1–Ag1–P1	101.55(4)
Ag2–Cl4	2.526(6)	Cl1–Ag1–P2	104.17(5)	Br1–Ag1–P2	103.66(3)	I1–Ag1–P2	111.54(5)	I1–Ag1–P2	112.12(4)
Ag3–Cl2	2.640(8)	Cl1–Ag1–P3	99.54(5)	Br1–Ag1–P3	99.95(3)	I1–Ag1–P3	99.44(5)	I1–Ag1–P3	98.57(3)
Ag3–Cl3	2.583(9)	P1–Ag1–P2	115.89(4)	P1–Ag1–P2	115.92(4)	P1–Ag1–P2	117.81(6)	P1–Ag1–P2	118.13(5)
Ag3–Cl4	2.780(8)	P1–Ag1–P3	108.40(4)	P1–Ag1–P3	108.06(3)	P1–Ag1–P3	111.94(6)	P1–Ag1–P3	111.87(5)
Ag4–Cl1	2.704(6)	P2–Ag1–P3	118.22(4)	P2–Ag1–P3	118.25(3)	P2–Ag1–P3	111.77(6)	P2–Ag1–P3	112.31(5)
Ag4–Cl3	2.709(9)								
Ag3–Cl4	2.780(8)								
Ag1–P1	2.384(8)								
Ag2–P2	2.394(8)								
Ag3–P3	2.394(5)								
Ag4–P4	2.403(10)								
Cl1–Ag1–Cl2	100.4(3)								
Cl1–Ag1–Cl3	94.4(2)								
Cl2–Ag1–Cl3	101.3(2)								
Cl1–Ag2–Cl2	92.8(3)								
Cl1–Ag2–Cl4	92.0(2)								
Cl2–Ag2–Cl4	98.5(2)								
Cl2–Ag3–Cl3	105.0(2)								
Cl2–Ag3–Cl4	93.8(2)								
Cl3–Ag3–Cl4	98.3(3)								
Cl1–Ag4–Cl3	92.0(2)								
Cl1–Ag4–Cl4	93.3(2)								
Cl3–Ag4–Cl4	100.3(3)								

Table 2
Cytostatic activity of complexes **1–4** as 50% inhibitory concentration (IC₅₀) values against sarcoma cancer cells (mesenchymal tissue) from the Wistar rat. water molecules

Complex	IC ₅₀ (μM)		
	24 h	48 hrs	72 h
1	0.825	0.750	0.750
2	0.650	0.750	0.750
3	0.750	0.640	0.750
4	0.850	0.800	0.750

Table 3
Inhibitory effects of complexes **1–4** as 50% inhibitory concentration (IC₅₀) on the proliferation of murine leukemia cells (L1210/0) and human T-lymphocyte cells (Molt4/C8, CEM/0)

Complex	IC ₅₀ * (μM)		
	L1210/0	Molt4/C8	CEM/0
1	28 ± 26	13 ± 3	2.5 ± 18
2	≥100	>100	≥100
3	1.8 ± 0.0	2.1 ± 0.1	2.3 ± 0.1
4	4.6 ± 3.1	2.7 ± 0.2	2.7 ± 0.5

139.80 ppm in **4**. Despite the fact that these shifts are not that large most probably due to a back donation effect [9a], they are nonetheless indicative of the coordination with the metal ion.

The ³¹P NMR spectrum of complex **1** shows one signal at 4.31 ppm while the spectra of complexes **3** and **4** show two resonance signals at 1.08 and at 27.05 ppm in case of **3** and at –4.34 and at 27.11 ppm in case of **4**. The presence of one resonance signal in the case of cubane like complex **1** indicate that the four phosphine ligands are equivalent in solution. In the case of complexes **3** and **4** with a tetrahedral geometry, however, the two signals observed, suggest that a ligand exchange equilibrium is established in solution of these complexes [9d], most probably because of the high steric effect of the bulky phosphine ligand.

2.3.3. Crystal and molecular structures of {[AgCl(tptp)]₄} (**1**), [AgCl(tptp)₃] (**2**), [AgBr(tptp)₃] (**3**) and [AgI(tptp)₃] (**4**)

Ortep diagrams of complexes **1–4** are shown in Figs. 1–4, while selected bond lengths and angles are given in Table 1.

Complex **1** (Fig. 1) consists of four Ag(I) ions bridged by μ₃-chloride ions, forming a cube like core. Thus, each Ag(I) ion is bonded with a tri-*p*-tolylphosphine (tptp) ligand through the phosphorus atom and three μ₃-Cl atoms forming a distorted tetrahedral arrangement around each metal center. The Ag–Cl bond length varies between 2.526 and 2.807 Å and are in agreement to those found in the cubane like complex [(Ph₃P)₄Ag₄Cl₄] (Ph₃P = triphenylphosphine) [11a] where Ag–Cl bond distances vary from 2.5316(25) to 2.7604(27) Å and in the dimeric complex [Ag(C₃₆H₃₀P₂)Cl]₂ [11b] where the two Ag–Cl bond distances are at 2.5472 and

2.7909 Å, respectively. The Ag–P bond lengths in complex **1** vary from 2.384 to 2.403 Å and are also in agreement to those found in complex $[(\text{Ph}_3\text{P})_4\text{Ag}_4\text{Cl}_4]$ [**11a**] (2.3755(27)–2.3878(26) Å). They are shorter, however, than the corresponding Ag–P bond distances found in the dimer $[\text{Ag}(\text{C}_{36}\text{H}_{30}\text{P}_2)\text{Cl}]_2$ (2.467(2)–2.472(2) Å) [**11b**] and significantly shorter than the Ag–P bond lengths found in the monomeric complexes **2**, **3** and **4** (2.53–2.56 Å) (Table 1) indicating a dependence on the geometry of the complex. A weak metal–metal interaction was found between Ag1–Ag3 and Ag3–Ag4 (3.280 and 3.435 Å, respectively) in complex **1**, which are shorter than the sum of their van der Waals radii (3.44 Å) indicating a d^{10} – d^{10} interaction [8a]. All the remaining Ag...Ag distances are longer than two-fold the value of van der Waals radii; Ag1...Ag2 = 3.548, Ag1...Ag4 = 3.631, Ag2...Ag3 = 3.537 and Ag2...Ag4 = 3.652 Å, respectively.

Complexes **2–4** (Figs. 2–4) are monomeric Ag(I) complexes with tetrahedral geometries around the metal ion formed by three P atoms from the ttp ligands and a halogen ion (X = Cl, Br, I). The Ag–P bond lengths vary from 2.53 to 2.56 Å and are in agreement with those found in the $[\text{Ag}(\text{Ph}_3\text{P})_3\text{Cl}]$ [**11c,11d**] complex (average Ag–P = 2.55 Å), in $[(\text{Ph}_3\text{P})\text{AgBr}]$ [**11d**] (average Ag–P = 2.54 Å), in $[(\text{Ph}_3\text{P})_3\text{AgI}]$ [**11d**] (average Ag–P = 2.63(1) Å), $[(\text{Ph}_3\text{P})_3\text{AgI}]$ [**12a**] (average Ag–P = 2.5913 Å) and $[(\text{Ph}_3\text{P})_3\text{AgI}]$ [**12b**] (average Ag–P = 2.60 Å) and in $[(\text{ttp})_3\text{AgI}]$ [8e] (Ag–P = 2.55 Å). No significant changes were observed between the structures of complex **4** solved at 140 or 293 K, indicating that the temperature has no effect on the complex conformation.

2.4. Biological tests

Complexes **1–4** were tested for *in vitro* cytostatic activity against sarcoma cancer cells (mesenchymal tissue) from the Wistar rat, polycyclic aromatic hydrocarbons (PAH, ben-

zo[*a*]pyrene) carcinogenesis. Table 2 presents the antiproliferative effects of complexes after treatment with variable concentration, at 24, 48 and 72 h exposure time, as 50% inhibitory concentration (IC_{50}) values. The corresponding (IC_{50}) value found for *cis*-platin, against sarcoma cancer cells (mesenchymal tissue) from the Wistar rats, is 4–5 μM [13a], while complexes **1–4** show a pronounced cytostatic activity against the tumor cell lines studied (see Table 2). The cytostatic activity of complexes **1–4**, was smaller than the corresponding ones found for organotin(IV)-thioamide complexes tested from our group with best results obtained with $\{[(\text{C}_6\text{H}_5)_3\text{Sn}]_2(\text{mna}) \cdot [(\text{CH}_3)_2\text{CO}]\}$ (H_2mna = 2-mercapto-nicotinic acid) (IC_{50} = 0.005 μM) [13a,13b], followed by $[(\text{C}_6\text{H}_5)_2\text{Sn}(\text{cmbzt})_2]$ (Hcmbzt = 5-chloro-2-mercapto-benzothiazole) (IC_{50} = 0.3–0.5 μM) [13c,13d] and $[(\text{C}_6\text{H}_5)_3\text{Sn}(\text{PMT})]$ (PMT = 2-mercapto-pyrimidine) (IC_{50} = 0.1 μM) [13c,13d].

Complexes **1–4** were also tested against murine leukemia (L1210) and human T-lymphocyte (Molt4/C8 and CEM) cells (Table 3). The values obtained show strong cytostatic activity with the bromide **3** and iodide **4** tetrahedral complexes to be the strongest. Complex **3**, also show stronger cytostatic activity against murine leukemia (L1210) and human T-lymphocyte (Molt4/C8 and CEM) cells than the silver(I)-thioamide complexes $\{[\text{Ag}_6(\mu_2\text{-Br})_6(\mu_2\text{-StpmH}_2)_4(\mu_3\text{-StpmH}_2)_2]_n\}$ and $\{[\text{Ag}_4(\mu_2\text{-StpmH}_2)_6(\text{NO}_3)_4]_n\}$ (StpmH_2 = 2-mercapto-3,4,5,6-tetrahydro-pyrimidine) tested previously [5].

All complexes were also tested for anti-HIV-1 and -HIV-2 activities, but were found inactive.

2.5. Computational study

The stability in the structure of **1** caused by cyclical delocalization of *d* as well as (*d*-*p*) π -type orbitals electron density, instead of the usual *p* orbitals on metal–ligand rings (*d* orbital aromaticity) [14], was calculated by mean of nucleus-independent chemical shifts (NICS) method. The

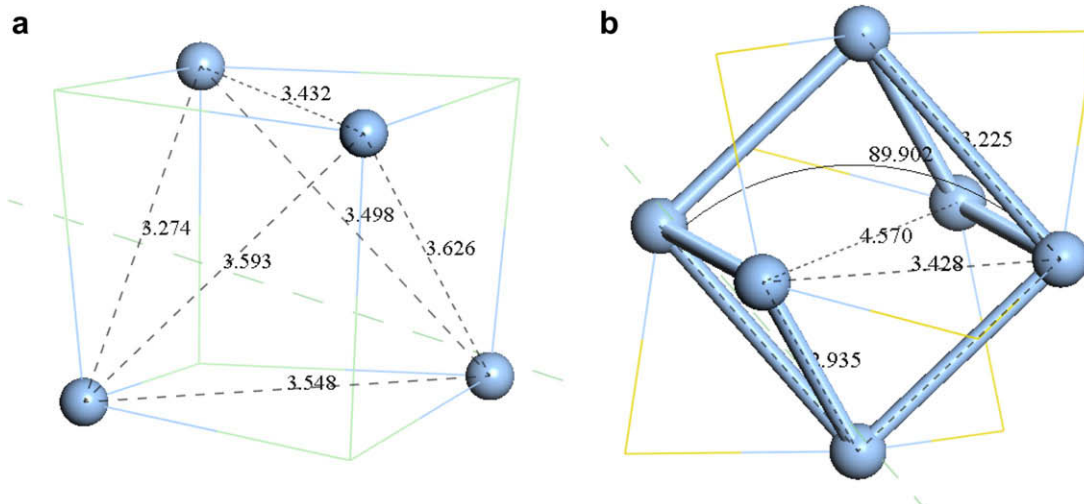


Fig. 5. Geometrical parameters for the core structures of compounds **1** and $\{[\text{Ag}_6(\mu_3\text{-Hmna})_4(\mu_3\text{-mna})_2]^{2-} \cdot [(\text{Et}_3\text{NH})^+]_2 \cdot (\text{DMSO})_2 \cdot (\text{H}_2\text{O})\}$ (**5**).

use of NICS method in 3D structures has been recently, evaluated extensively [14e,14d] showing the successful estimation of aromaticity. In this work the NICS values have been calculated for complex **1** at: (i) special positions located at the centre of the plane determined by the three nearest Ag atoms (NICS-3Ag) where Ag··Ag contacts are shorter than the sum of van der Waals radii (Fig. 5a) (−2.4 ppm) and at (ii) the cage centres (NICS(0.0)) (−0.2 ppm). For comparison we extended our calculation on the $\{[\text{Ag}_6(\mu_3\text{-Hmna})_4(\mu_3\text{-mna})_2]^{2-} \cdot [(\text{Et}_3\text{NH})^+]_2 \cdot (\text{DM-SO})_2 \cdot (\text{H}_2\text{O})\}$ (**5**) complex [15] (NICS-3Ag = −5.5 ppm and NICS(0.0) = 0.2, respectively (Fig. 5b)) and on benzene (NICS(0.0) = −6.9 ppm) and the recently calculated $\{[\text{Ag}_4\text{Cl}_4(\mu_3\text{-StpmH}_2)_4]_n\}$ aggregate [14f], (NICS = −9.7 ppm), at the same level of theory. The core of complex **1** exhibits pseudo-tetrahedral (T_d) symmetry while the cores of complex **5** and C_6H_6 adopt D_{3d} and D_{6h} symmetry, respectively. These results show aromaticity in the special position at the centre of the plane established by the three nearest Ag atoms in cases of **1** and **5**. However, the aromaticity calculated in complex **1** is significantly lower than the corresponding found in the nano-tube shaped $\{[\text{Ag}_4\text{Cl}_4(\mu_3\text{-StpmH}_2)_4]_n\}$ aggregate [14f] where the NICS data of −9.7 ppm at the cage barycentre confirmed a strong aromatic character. Shielding influence reached its minimum value of −13.1 ppm at NICS(1.7) [14f].

3. Conclusions

Four new Ag(I) complexes were synthesized by reacting silver halogenides and tri-*p*-tolyl-phosphine. The geometry is found to depend on the stoichiometry of the reaction. Thus, the 1:1 ligand to metal ratio leads to the formation of the cubane $\{[\text{AgCl}(\text{tptp})]_4\}$ (**1**), while the 1:3 ratio results in the formation of the tetrahedral complexes, $[\text{AgX}(\text{tptp})_3]$ (X = Cl (**2**), Br (**3**), I (**4**)). The formation of the cubane like complex **1** may be explained by the aromaticity calculated at special positions located at the centre of the plane determined by the three nearest Ag atoms (NICS-3Ag), which may give extra stability to this structure. This may also explain the weak Ag··Ag ($d^{10}\text{--}d^{10}$) interaction found between Ag1–Ag3 and Ag3–Ag4 (3.276 and 3.444 Å, respectively), which are shorter than the sum of their van der Waals radii (3.44 Å). The IC_{50} values of complexes **1–4**, against sarcoma cancer cells, vary from 0.650 to 0.850 μM with the corresponding value for cisplatin to be 4–5 μM [13a], but weaker than that of organotin(IV)–thioamide complexes [13a,13b,13c,13d]. Complexes **1–4** also show strong cytostatic activity against murine leukemia (L1210) and human T-lymphocyte (Molt4/C8 and CEM) cells (Table 3). This activity is higher than that of the corresponding silver(I)–thioamide complexes $\{[\text{Ag}_6(\mu_2\text{-Br})_6(\mu_2\text{-StpmH}_2)_4(\mu_3\text{-StpmH}_2)_2]_n\}$ and $\{[\text{Ag}_4(\mu_2\text{-StpmH}_2)_6(\text{NO}_3)_4]_n\}$ (StpmH₂ = 2-mercapto-3,4,5,6-tetrahydro-pyrimidine) [5]. Iodine **4** and bromine **3** silver(I) complexes with tetrahedral geometry show significantly stronger cytostatic activity than the corresponding chlorides, while between

the chlorides of **1** and **2** complexes stronger cytostatic activity is found for complex **2** with tetrahedral geometry than that of **1** with the cubane structure. This may be explained by the aromaticity calculated at special positions located at the centre of the plane determined by the three nearest Ag atoms (NICS-3Ag) in case of complex **1**, which may give extra stability to this structure. Finally none of the complexes show anti HIV activity.

4. Experimental

4.1. Materials and instruments

All solvents used were of reagent grade. Silver(I) chloride and Silver(I) bromide were prepared by mixing aqueous solutions of AgNO_3 with the appropriate amount of NaCl and NaBr (Merck or Aldrich), respectively. The precipitations were filtered off and dried on a filtering paper in darkness. Silver(I) iodide (Fluka AG, Buchs SG) was of analytical reagent. Tri-*p*-tolyl-phosphine (Fluka) was used with no further purification. Elemental Analyses for C, H, N, were carried out with a Carlo Erba EA model 1108 elemental analyzer. Melting points were measured in open tubes with a Stuart Scientific apparatus and are uncorrected. IR spectra in the region of 4000–370 cm^{-1} were obtained from KBr discs, while far-IR spectra in the region 400–30 cm^{-1} were obtained from polyethylene discs, with a Perkin–Elmer Spectrum GX FT-IR spectrophotometer. The ^1H and ^{13}C NMR spectra were recorded on a Bruker AC250 MHFT NMR instrument in CDCl_3 solutions. Chemical Shifts are given in ppm referenced to internal TMS. The ^{31}P NMR spectra were recorded in CD_3CN solutions.

4.2. Synthesis and crystallization of $\{[\text{AgC}(\text{tptp})]_4\}$ (**1**), $[\text{AgCl}(\text{tptp})_3]$ (**2**), $[\text{AgBr}(\text{tptp})_3]$ (**3**) and $[\text{AgI}(\text{tptp})_3]$ (**4**)

A 20 ml of $\text{CH}_3\text{OH}/\text{CH}_3\text{CN}$ (1:1) solution of tri-*p*-tolyl-phosphine (tptp) (0.153 g 0.5 mmol) with 0.5 mmol silver(I) salt (AgCl, 0.073 g, or AgBr, 0.095 g or AgI, 0.117 g) was stirred for 15 min at 50 °C. In case of complex **2** the 20 ml $\text{CH}_3\text{OH}/\text{CH}_3\text{CN}$ (1:1) solution of tri-*p*-tolyl-phosphine (tptp) (0.153 g 0.5 mmol) and AgCl (0.0036 g 0.17 mmol) was stirred under reflux until clearness. The resultant suspensions were filtered off and the filtrates were kept in darkness at room temperature. After few days colorless crystals of complexes were obtained; suitable for X-ray crystallographic.

1: Yield: 0.020 g; m.p.: 235–244 °C; ($\text{C}_8\text{H}_8\text{P}_4\text{Ag}_4\text{Cl}_4$) (1789.4); Anal. Calc.: C, 56.34; H, 4.72. Found: C, 56.64; H, 5.18%. MID-IR (cm^{-1}) (KBr): 3030w, 2189w, (1925–1908)w, 1596m, 1497s, 1397s, 1310m, 1188vs, 1097vs, 806vs, 708s, 643s, 629vs, 610s, 512vs, 424m, 375m. FAR-IR (cm^{-1}) (pe): 186w, 136w, 113w. UV–is (λ_{max} nm, log ϵ), (CHCl_3), ($C = 1 \times 10^{-5}$ M): $\lambda_{\text{max}_1} = 250$, log $\epsilon = 4.851$, $\lambda_{\text{max}_2} = 242$, log $\epsilon = 4.854$, UV–is (λ_{max} nm, log ϵ), (MeOH).

Table 4
Crystal data and the structure refinement details for the complexes 1–4

	1; 293 K	2; 293 K	3; 293 K	4; 293 K	4; 140 K
Empirical formula	C ₈₄ H ₈₄ Ag ₄ Cl ₄ P ₄	C ₆₃ H ₆₃ AgClP ₃	C ₆₃ H ₆₃ AgBrP ₃	C ₆₃ H ₆₃ AgIP ₃	C ₆₃ H ₆₃ AgIP ₃
Formula weight	1790.68	1056.36	1100.82	1146.81	1146.81
Temperature (K)	100(1)	293(2)	293(2)	293(2)	140(2)
Crystal system	triclinic	orthorhombic	orthorhombic	triclinic	triclinic
Space group	<i>P</i> 1	<i>Pna</i> 21	<i>Pna</i> 21	<i>P</i> $\bar{1}$	<i>P</i> $\bar{1}$
<i>a</i> (Å)	12.752(2)	20.5161(9)	20.487(4)	11.038(2)	11.0058(5)
<i>b</i> (Å)	13.014(2)	26.3246(12)	26.186(5)	11.548(2)	11.4509(5)
<i>c</i> (Å)	15.094(2)	10.6442(7)	10.674(2)	23.227(5)	22.9459(8)
α (°)	80.491(13)	90	90	99.29(3)	99.461(3)
β (°)	66.165(16)	90	90	92.12(3)	91.648(3)
γ (°)	61.602(17)	90	90	106.19(3)	106.350(4)
<i>V</i> (Å ³)	2014.4(5)	5748.7(5)	5726.3(19)	2795.4(11)	2728.5(2)
<i>Z</i>	1	4	4	2	2
ρ_{calcd} (g cm ⁻³)	1.476	1.221	1.277	1.362	1.396
μ (mm ⁻¹)	1.21	0.5	1.2	1.0	1.1
<i>R</i> , <i>wR</i> ₂ [<i>I</i> > 2 σ (<i>I</i>)]	0.0793, 0.1972	0.0483, 0.1282	0.0463, 0.1094	0.0546, 0.1691	0.0687, 0.1867

(*C* = 1 × 10⁻⁵ M): λ_{max} = 250, log ϵ = 4.804. ¹H NMR (δ ppm), (CDCl₃): 2.34(s), 7.31(d), 7.1(d), ¹³C NMR (δ ppm) (CDCl₃): 21.88, 77.51, 134.2, 130, 140.5. Conductivity (*A*_m) in CH₃CN = 1 cm⁻¹ mol⁻¹ Ω ⁻¹.

2: Yield: 0.084 g; m.p: 175–177 °C (C₆₃H₆₃P₃AgCl) (1055.4) *Anal. Calc.:* C, 71.70; H, 5.97. Found: C, 71.70; H, 5.96%. MID-IR (cm⁻¹) (KBr): 3013m, 1916m, 1595m, 1498s, 1396m, 1308m, 1189s, 1090s, 847w, 710m, 640w, 623m, 604w, FAR-IR (cm⁻¹) (pe): 172w, 151m, UV–is (λ_{max} nm, log ϵ), (CHCl₃), (*C* = 2 × 10⁻⁵ M): $\lambda_{\text{max}1}$ = 251, log ϵ = 4.745, $\lambda_{\text{max}2}$ = 243, log ϵ = 4.747, UV–is (λ_{max} nm, log ϵ), (MeOH), (*C* = 2 × 10⁻⁵ M): λ_{max} = 254, log ϵ = 4.532, ¹H NMR (δ ppm), (CDCl₃): 2.2–2.33(s), 7.3(d), 7.1(d), ¹³C NMR (δ ppm) (CDCl₃): 21.37, 77, 134, 129.5, 139.5. Conductivity (*A*_m) in CH₃CN = 14 cm⁻¹ mol⁻¹ Ω ⁻¹.

3: Yield: 0.073 g; m.p: 178–186 °C; (C₆₃H₆₃P₃AgBr) (1099.8) *Anal. Calc.:* C, 68.74; H, 5.76. Found: C, 68.85; H, 6.12%. MID-IR (cm⁻¹) (KBr): 3020m, 1910m, 1803w, 1597s, 1498s, 1396s, 1377w, 1309s, 1189s, 1095s, 851–840w, 806vs, 708vs, 642vs, 628vs, 609vs, 517–508vs, 427m, 410m. FAR-IR (cm⁻¹) (pe): 135w. UV–is (λ_{max} nm, log ϵ), (CHCl₃), (*C* = 2 × 10⁻⁵ M): $\lambda_{\text{max}1}$ = 253, log ϵ = 4.677 $\lambda_{\text{max}2}$ = 242, log ϵ = 4.674, UV–is (λ_{max} nm, log ϵ), (MeOH) (*C* = 2 × 10⁻⁵ M): λ_{max} = 253, log ϵ = 4.404, ¹H NMR (δ ppm), (CDCl₃): 2.34(s), 7.31(d), 7.1(d), ¹³C NMR (δ ppm) (CDCl₃): 21.40, 77, 133.74, 129.5, 147.5. Conductivity (*A*_m) in CH₃CN = 7 cm⁻¹ mol⁻¹ Ω ⁻¹.

4: Yield: 0.081 g; m.p: 158–163 °C; (C₆₃H₆₃P₃AgI) (1146.8); *Anal. Calc.:* C, 65.92; H, 5.53. Found: C, 65.9; H, 5.78%. MID-IR (cm⁻¹) (KBr): 3021w, 1910w, 1597m, 1497s, 1189s, 1121w, 1092vs, 1035w, 803vs, 706s, 642m, 628s, 608s, 508w, 430m, 418w, FAR-IR (cm⁻¹) (pe): 151s, 125m, UV–is (λ_{max} nm, log ϵ), (CHCl₃), (*C* = 2 × 10⁻⁵ M): $\lambda_{\text{max}1}$ = 253, log ϵ = 4.611, $\lambda_{\text{max}2}$ = 240, log ϵ = 4.656, UV–is (λ_{max} nm, log ϵ) (MeOH), (*C* = 2 × 10⁻⁵ M): λ_{max} = 258, log ϵ = 4.566, ¹H NMR (δ ppm), (CDCl₃): 2.33(s), 7.3(d), 7.1(d), ¹³C NMR (δ ppm)

(CDCl₃): 21.42, 77.0, 134, 129.5, 139.7. Conductivity (*A*_m) in CH₃CN = 11 cm⁻¹ mol⁻¹ Ω ⁻¹.

4.3. Cytostatic, antiviral activity assays and computational details

These have been described in detail elsewhere [5,13,14f].

4.4. X-ray structure determination

Intensity data for the colourless crystals of 1–4 were collected by the ω scan technique in the θ – 2θ range of range 2–60 for 1 at 100 K and 0.00 + 0.35 for 2–4 at 293 K and at 140 K temperature for 4 on a KUMA KM4CCD four-circle diffractometer [16a] with CCD detector, using graphite-monochromated MoK α (λ = 0.71073 Å) at 293(2) K. Cell parameters were determined by a least-squares fit [16b]. All data were corrected for Lorentz-polarization effects and absorption [16b,16c].

The structure was solved with direct methods with SHELXS97 [16d] and refined by full-matrix least-squares procedures on *F*² with SHELXL97 [16e]. All non-hydrogen atoms were refined anisotropically, hydrogen atoms were located at calculated positions and refined as a ‘riding model’ with isotropic thermal parameters fixed at 1.2 times the *U*_{eq}’s of appropriate carrier atom. Significant crystal data are given in Table 4.

5. Supplementary material

CCDC 622155, 622156, 622157, 622158, and 622159 contain the supplementary crystallographic data for 1, 2, 3, 4 and 4 at 140 K. These data can be obtained free of charge via <http://www.ccdc.cam.ac.uk/conts/retrieving.html>, or from the Cambridge Crystallographic Data Centre, 12 Union Road, Cambridge CB2 1EZ, UK; fax: (+44) 1223-336-033; or e-mail: deposit@ccdc.cam.ac.uk.

Acknowledgement

This work was carried out in partial fulfillment of the requirements for an M.Sc. thesis of Mr S.Z. within the graduate program in Bioinorganic Chemistry.

References

- [1] (a) P.G. Blower, J.R. Dilworth, *Coord. Chem Rev.* 76 (1987) 121;
(b) E.S. Raper, *Coord. Chem.* 61 (1985) 115;
(c) E.S. Raper, *Coord. Chem. Rev.* 129 (1994) 91;
(d) E.S. Raper, *Coord. Chem. Rev.* 153 (1996) 199.
- [2] (a) Martidale, *The Extra Pharmacopoeia*, 28th ed., The Pharmaceutical Press, London, 1982;
(b) M. Wruble, *J. Am. Pharm. Assoc. Sci. Ed.* 32 (1943) 80.
- [3] H.S. Rosenkranz, S. Rosenkranz, *Antimicrob. Agents Chemother.* 2 (1972) 373.
- [4] E.E. Tredget, H.A. Shankowsky, A. Groenveld, R. Burrell, *Burn Care Rehabil.* 19 (1998) 531.
- [5] P.C. Zachariadis, S.K. Hadjikakou, N. Hadjiliadis, A. Michaelides, S. Skoulika, J. Balzarini, E. De Clercq, *Eur. J. Inorg. Chem.* (2004) 1420.
- [6] (a) J.J. Roberts, J.M. Pascoe, *Nature* 235 (1972) 282;
(b) D.R. Williams, *Educ. Chem.* 11 (1974) 124.
- [7] (a) J. Vicente, M.T. Chicote, C. Rubio, *Chem. Ber.* 129 (1996) 327;
(b) J. Vicente, M.T. Chicote, M.C. Lagunas, *Inorg. Chem.* 32 (1993) 3748;
(c) O. Steigelmann, P. Bissinger, H. Schmidbaur, *Angew. Chem. Int. Ed.* 29 (1990) 1399;
O. Steigelmann, P. Bissinger, H. Schmidbaur, *Angew. Chem.* 102 (1990) 1473;
(d) B.P. Esposito, R. Najjar, *Coord. Chem. Rev.* 232 (2002) 137;
(e) M.J. McKeage, L. Maharaj, S.J. Berners-Price, *Coord. Chem. Rev.* 232 (2002) 127;
(f) M.D. Rhodes, P.J. Sadler, M.D. Scawen, S. Silver, *J. Inorg. Biochem.* 46 (1992) 129.
- [8] (a) K. Nomiya, S. Takahashi, R. Noguchi, *J. Chem. Soc., Dalton Trans.* (2000) 2091;
(b) K. Nomiya, R. Noguchi, T. Shigeta, Y. Kondoh, K. Tsuda, K. Ohsawa, N.C. Kasuga, M. Oda, *Bull. Chem. Soc. Jpn.* 73 (2000) 1143;
(c) P. Aslanidis, P.J. Cox, S. Divanidis, P. Karagiannidis, *Inorg. Chim. Acta* 357 (2004) 2677;
(d) P.J. Cox, P. Aslanidis, P. Karagiannidis, S.K. Hadjikakou, *Inorg. Chim. Acta* 310 (2000) 268;
(e) R. Meijboom, *Acta Cryst.* E63 (2007) m78.
- [9] (a) R.N. Dash, D.V. Ramana Rao, *Z. Anorg. Allg. Chem.* 393 (1972) 309;
(b) W. McFarlane, P.D. Akrivos, P. Aslanidis, P. Karagiannidis, C. Hatzisymeon, M. Newman, S. Kokkou, *Inorg. Chim. Acta* 281 (1998) 121;
(c) S. Attar, N.W. Alcock, G.A. Bowmaker, J.S. Frye, W.H. Bearden, J.H. Nelson, *Inorg. Chem.* 30 (1991) 4166;
(d) E.L. Muetterties, C.W. Alegranti, *J. Am. Chem. Soc.* 94 (1972) 6386.
- [10] (a) I. Krossing, L. van Wullen, *Chem. Eur. J.* 8 (2002) 700;
(b) G.A. Bowmaker, Effendy, J.V. Hanna, P.C. Healy, B.W. Skelton, A.H. White, *J. Chem. Soc., Dalton Trans.* (1993) 1387.
- [11] (a) B-K. Teo, J.C. Calabrese, *Inorg. Chem.* 15 (1976) 2467;
(b) A. Cassel, *Acta Cryst.* B35 (1979) 174;
(c) A. Cassel, *Acta Cryst.* B37 (1981) 229;
(d) L.M. Engelhardt, P.C. Healy, V.A. Patrick, A.H. White, *Aust. J. Chem.* 40 (1987) 1873.
- [12] (a) D.E. Hibbs, M.B. Hursthouse, K.M. Abdul-Malik, M.A. Beckett, P.W. Jones, *Acta Cryst.* C52 (1996) 884;
(b) M. Camali, F. Caruso, *Inorg. Chim. Acta* 127 (1987) 209.
- [13] (a) M.N. Xanthopoulou, S.K. Hadjikakou, N. Hadjiliadis, M. Schürmann, K. Jurkschat, J. Binolis, S. Karkabounas, K. Charalabopoulos, *Bioinorg. Chem. Appl.* 1 (2003) 227;
(b) M.N. Xanthopoulou, S.K. Hadjikakou, N. Hadjiliadis, M. Schürmann, K. Jurkschat, A. Michaelides, S. Skoulika, T. Bakas, J. Binolis, S. Karkabounas, K. Haralampopoulos, *J. Inorg. Biochem.* 96 (2003) 425;
(c) M.N. Xanthopoulou, S.K. Hadjikakou, N. Hadjiliadis, M. Kubicki, S. Skoulika, T. Bakas, M. Baril, I.S. Butler, *Inorg. Chem.* 46 (2007) 1187;
(d) M.N. Xanthopoulou, S.K. Hadjikakou, N. Hadjiliadis, E.R. Milaeva, J.A. Gracheva, V.-Y. Tyurin, N. Kourkoumelis, K.C. Christoforidis, A.K. Metsios, S. Karkabounas, K. Charalabopoulos, *Eur. J. Med. Chem.*, in press, doi:10.1016/j.ejmech.2007.03.028.
- [14] (a) P.v.R. Schleyer, C. Maerker, A. Dransfeld, H. Jiao, N.J.R.v.E. Hommes, *J. Am. Chem. Soc.* 118 (1996) 6317;
(b) C. Corminboeuf, C.S. Wannere, D. Roy, R.B. King, P.v.R. Schleyer, *Inorg. Chem.* 45 (2006) 214;
(c) C.A. Tsipis, *Coord. Chem. Rev.* 249 (2005) 2740;
(d) J. Li, C.-W. Liu, J.-X. Lu, *J. Cluster Sci.* 7 (1996) 469;
(e) Z. Chen, R.B. King, *Chem. Rev.* 105 (2005) 3613;
(f) S. Zartilas, N. Kourkoumelis, S.K. Hadjikakou, N. Hadjiliadis, P. Zachariadis, M. Kubicki, A.-Y. Denisov, I.S. Butler, *Eur. J. Inorg. Chem.* (2007) 1219.
- [15] P.C. Zachariadis, S.K. Hadjikakou, N. Hadjiliadis, A. Michaelides, S. Skoulika, Y. Ming, Y. Xiaolin, *Inorg. Chim. Acta* 343 (2003) 361.
- [16] (a) KUMA KM-4CCD user manual, KUMA Diffraction, Wroclaw, Poland, 1999;
(b) CRYCALIS, Program for Reduction of the Data from KUMA CCD Diffractometer, KUMA Diffraction, Wroclaw, Poland, 1999;
(c) R.H. Blessing, *J. Appl. Crystallogr.* 22 (1989) 396;
(d) G.M. Sheldrick, *Acta Cryst.* A 46 (1990) 467;
(e) G.M. Sheldrick, SHELXL-97, Program for the Refinement of Crystal Structures, University of Göttingen, Göttingen, Germany, 1997.